Redox Biology 12 (2017) 300–310

Contents lists available at ScienceDirect

Redox Biology

journal homepage: www.elsevier.com/locate/redox

Research Paper

Polychlorinated biphenyls-153 induces metabolic dysfunction through activation of ROS/NF-κB signaling via downregulation of HNF1b

Hao Wu[1], Weihua Yu[1], Fansen Meng, Jie Mi, Jie Peng, Jiangzheng Liu, Xiaodi Zhang, Chunxu Hai*, Xin Wang*

Department of Toxicology, Shaanxi Key Lab of Free Radical Biology and Medicine, the Ministry of Education Key Lab of Hazard Assessment and Control in Special Operational Environment, School of Public Health, Fourth Military Medical University, Xi'an 710032, China

ARTICLE INFO

Keywords:
Polychlorinated biphenyls
Glucose and lipid metabolic disorder
Hepatocyte nuclear factor 1b
Reactive oxygen species
NF-κB

ABSTRACT

Polychlorinated biphenyls (PCB) is a major type of persistent organic pollutants (POPs) that act as endocrine-disrupting chemicals. In the current study, we examined the mechanism underlying the effect of PCB-153 on glucose and lipid metabolism in vivo and in vitro. We found that PCB-153 induced per se and worsened high fat diet (HFD)-resulted increase of blood glucose level and glucose and insulin intolerance. In addition, PCB-153 induced per se and worsened HFD-resulted increase of triglyceride content and adipose mass. Moreover, PCB-153 concentration-dependently inhibited insulin-dependent glucose uptake and lipid accumulation in cultured hepatocytes and adipocytes. PCB-153 induced the expression and nuclear translocation of p65 NF-κB and the expression of its downstream inflammatory markers, and worsened HFD-resulted increase of those inflammatory markers. Inhibition of NF-κB significantly suppressed PCB-153-induced inflammation, lipid accumulation and decrease of glucose uptake. PCB-153 induced oxidative stress and decreased hepatocyte nuclear factor 1b (HNF1b) and glutathione peroxidase 1 (GPx1) expression in vivo and in vitro. Overexpression of HNF1b increased GPx1 expression, decreased ROS level, decreased Srebp1, ACC and FAS expression, and inhibited PCB-153-resulted oxidative stress, NF-κB-mediated inflammation, and final glucose/lipid metabolic disorder. Our results suggest that dysregulation of HNF1b/ROS/NF-κB plays an important role in PCB-153-induced glucose/lipid metabolic disorder.

1. Introduction

In the last decades, the prevalence of diabetes and related diseases of metabolic disorders has a dramatic increase [1]. It is estimated that the prevalence of diabetes for all age-groups worldwide will be 4.4% and the total number of diabetes patients is projected to rise to 366 million in 2030 [1]. Being the fifth leading cause of death, diabetes contributed to 5.2% of all deaths in 2000 [2]. In developed Europe, over one in five people meets the criteria for either impaired glucose tolerance, increased fasting glucose or both [3].

The global prevalence of diabetes and its related diseases is closely associated with the exposure to environmental risks [4,5]. Persistent organic pollutants (POPs) is an important environmental pollutant that is resistant to degradation in the environment and highly persistent in the human body [6,7]. High storage of POPs is linked with diabetes risk [8–11]. Polychlorinated biphenyls (PCBs) is a main type of POPs [12]. Clinical and experimental evidence has shown that exposure to PCBs is linked with obesity and diabetes [12–16]. Significant associations between elevated PCB levels and diabetes has been observed in human body [17]. Chronic exposure to PCBs has been shown to exacerbate obesity-induced insulin resistance and hyperinsulinemia in mice [15]. In high fat diet (HFD)-fed mice, PCB-153 acts as an obesogen that exacerbates hepatic steatosis, alters adipocytokines and disrupts normal hepatic lipid metabolism [18]. However, the mechanism of PCB-induced negative effect on glucose and lipid metabolism is far from completely understood.

Diabetes is characterized by increased oxidative stress and inflammation. However, the role of oxidative stress and inflammation in PCB-induced metabolic disorder is unclear. In the current study, we aimed to investigate the mechanism underlying PCB-resulted insulin resistance and to focus on oxidative stress and inflammation-related molecular mechanism. We showed that downregulation of hepatocyte nuclear factor 1b (HNF1b), a novel redox regulator, played a crucial role in PCB-153-induced oxidative stress. PCB-153 reduced HNF1b

* Corresponding authors.
E-mail address: xinwang@fmmu.edu.cn (X. Wang).
[1] Coauthors.

http://dx.doi.org/10.1016/j.redox.2017.02.026
Received 7 February 2017; Received in revised form 25 February 2017; Accepted 28 February 2017
Available online 07 March 2017

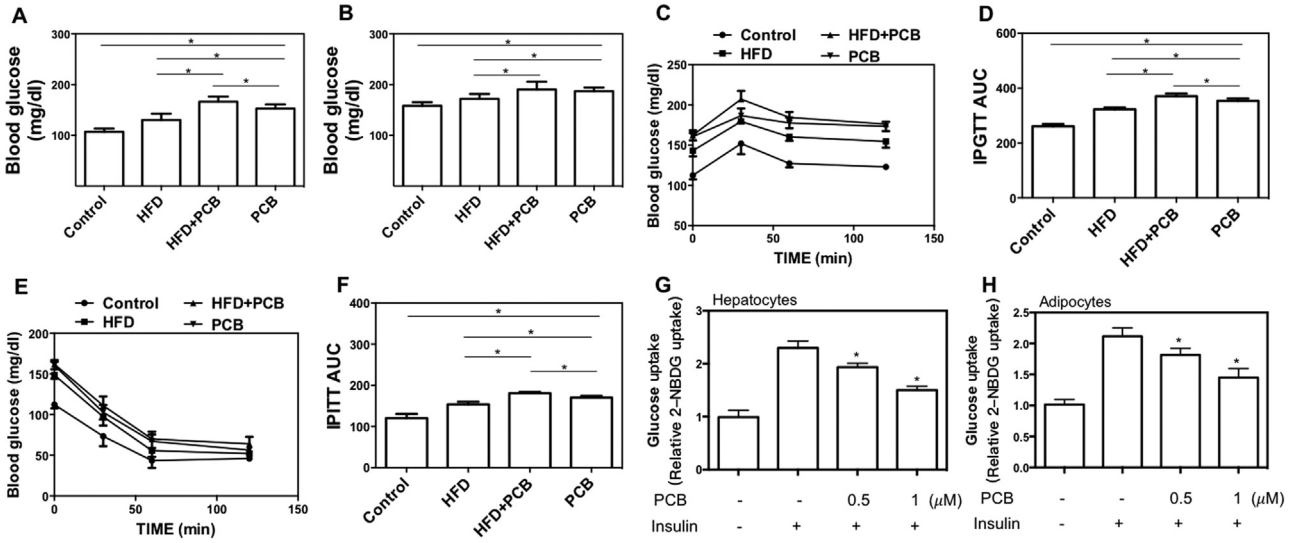

Fig. 1. Effect of PCB-153 on glucose metabolism in vivo and in vitro. Mice were fed high fat diet (HFD) and drank water containing PCB-153. At the end of the experiment, fasting (A) and refed (B) blood glucose level was determined using a glucometer. IPGTT was conducted to evaluate glucose tolerance activity (C) and area under the curve was calculated (D). IPITT was conducted to evaluate insulin tolerance activity (E) and AUC was calculated (F). *$p < 0.05$, significant differences between the two groups. AML-12 hepatocytes were treated by 0.5 and 1 μM PCB-153 for 24 h and the insulin-stimulated glucose uptake was evaluated and shown as folds of control (E). Differentiated 3T3-L1 adipocytes were treated by 0.5 and 1 μM PCB-153 for 24 h and the insulin-stimulated glucose uptake was evaluated and shown as folds of control (F). *$p < 0.05$, significant differences compared with control.

expression, elevated reactive oxygen species (ROS) level, and enhanced NF-κB-mediated inflammation, resulting in abnormal accumulation of lipid and disorder of glucose metabolism.

2. Results

2.1. PCB-153 resulted in glucose metabolic dysfunction

To investigate the effect of PCB-153 exposure on glucose/lipid metabolism, mice were administrated with PCB-153 alone or in combination with HFD. PCB-153 induced and worsened HFD-induced increase in body weight (Supplemental Fig. 1). PCB-153 administration resulted in a significant increase in fasting blood glucose level and refed blood glucose level which was higher than that of HFD group (Fig. 1A and B). Moreover, PCB-153 aggravated HFD-resulted increase of fasting blood glucose level (Fig. 1A). The blood glucose level in IPGTT and IPITT tests was markedly increased by PCB-153, which was notably higher than that in HFD group (Fig. 1C, D, E and F), indicating the impairment of glucose and insulin tolerance. Furthermore, the glucose and insulin intolerance in HFD group was worsened by PCB-153 (Fig. 1C, D, E and F). In AML-12 hepatocytes and 3T3-L1 adipocytes, insulin-stimulated glucose uptake was inhibited by PCB-153 in a concentration-dependent manner (Fig. 1G and H). These results demonstrated that PCB-153 could not only worsen HFD-resulted glucose metabolic dysfunction but also result in abnormal glucose metabolism per se.

2.2. PCB-153 resulted in abnormal lipid accumulation

Disorder of lipid metabolism plays a fundamental role in glucose metabolic dysfunction. In the next step, we tested the effect of PCB-153 lipid metabolism. PCB-153 administration induced a significant increase in serum and liver triglyceride (TG) content, epididymal fat weight and adipocyte size in mice (Fig. 2A, B, C and D), which was higher than that of HFD group. Moreover, HFD-resulted increase in serum and liver TG content, epididymal fat weight and adipocyte size were markedly worsened by PCB-153 (Fig. 2A, B, C and D). PCB-153 treatment concentration-dependently increased lipid droplets and TG content in AML-12 cells and 3T3-L1 adipocytes in vitro (Fig. 2E, F, G and H). These results demonstrated that PCB-153 could not only worsen HFD-resulted lipid metabolic disorder but also result in abnormal lipid accumulation per se.

2.3. NF-κB-mediated inflammation was involved in PCB-153-resulted glucose/lipid metabolic disorder

Inflammation is a critical pathophysiological process in the development of lipid/glucose metabolic disorder. The effect of PCB-153 on inflammation was evaluated in the study. As shown in Fig. 3A-D, PCB-153 resulted in a significant increase in the mRNA expression and nuclear protein expression of p65 NF-κB and mRNA expression of IL-1α and IL-6, and decrease of cytoplasmic expression of p65 NF-κB in livers of mice. In addition, PCB-153 worsened HFD-resulted increase of mRNA expression and nuclear protein expression of p65 NF-κB, and mRNA expression of IL-1α and IL-6 in livers and decrease of cytoplasmic expression of p65 NF-κB (Fig. 3A-D). In adipose tissues of mice, PCB-153 significantly increased the mRNA expression of p65 NF-κB and IL-1α and nuclear protein expression of p65 NF-κB, and decreased cytoplasmic expression of p65 NF-κB (Fig. 3E-G). Moreover, PCB-153 worsened HFD-resulted increase of p65 NF-κB, IL-1α, and IL-6 mRNA expression and nuclear p65 NF-κB protein expression, and decrease of cytoplasmic expression of p65 NF-κB in adipose tissues (Fig. 3E-H). In both AML-12 hepatocytes and 3T3-L1 adipocytes, PCB-153 resulted in a significant increase in the mRNA expression of p65 NF-κB, IL-1α, and IL-6 and nuclear protein expression of p65 NF-κB, and a marked decrease of cytoplasmic expression of p65 NF-κB (Fig. 3I-P). These results demonstrated that PCB-153 could not only worsen HFD-resulted increase of inflammatory markers but also result in NF-κB-mediated inflammation per se.

To test whether the inflammation was involved in PCB-153-induced glucose/lipid metabolic dysfunction, AML-12 hepatocytes and 3T3-L1 adipocytes were treated with PCB-153 in the presence of BMS-345541 or pyrrolidine dithiocarbamate (PDTC), inhibitors of NF-κB activity. BMS-345541 and PDTC significantly reduced basal and PCB-153-induced increase of IL-1α mRNA expression in hepatocytes and adipocytes (Fig. 4A and B, Supplemental Fig. 2A and B). PCB-153-induced increase of TG content in hepatocytes and adipocytes was inhibited by BMS-345541 and PDTC treatment (Fig. 4A and B, Supplemental Fig. 2A and B), indicating that NF-κB-mediated inflammation was involved in PCB-153-induced lipid accumulation. PCB-

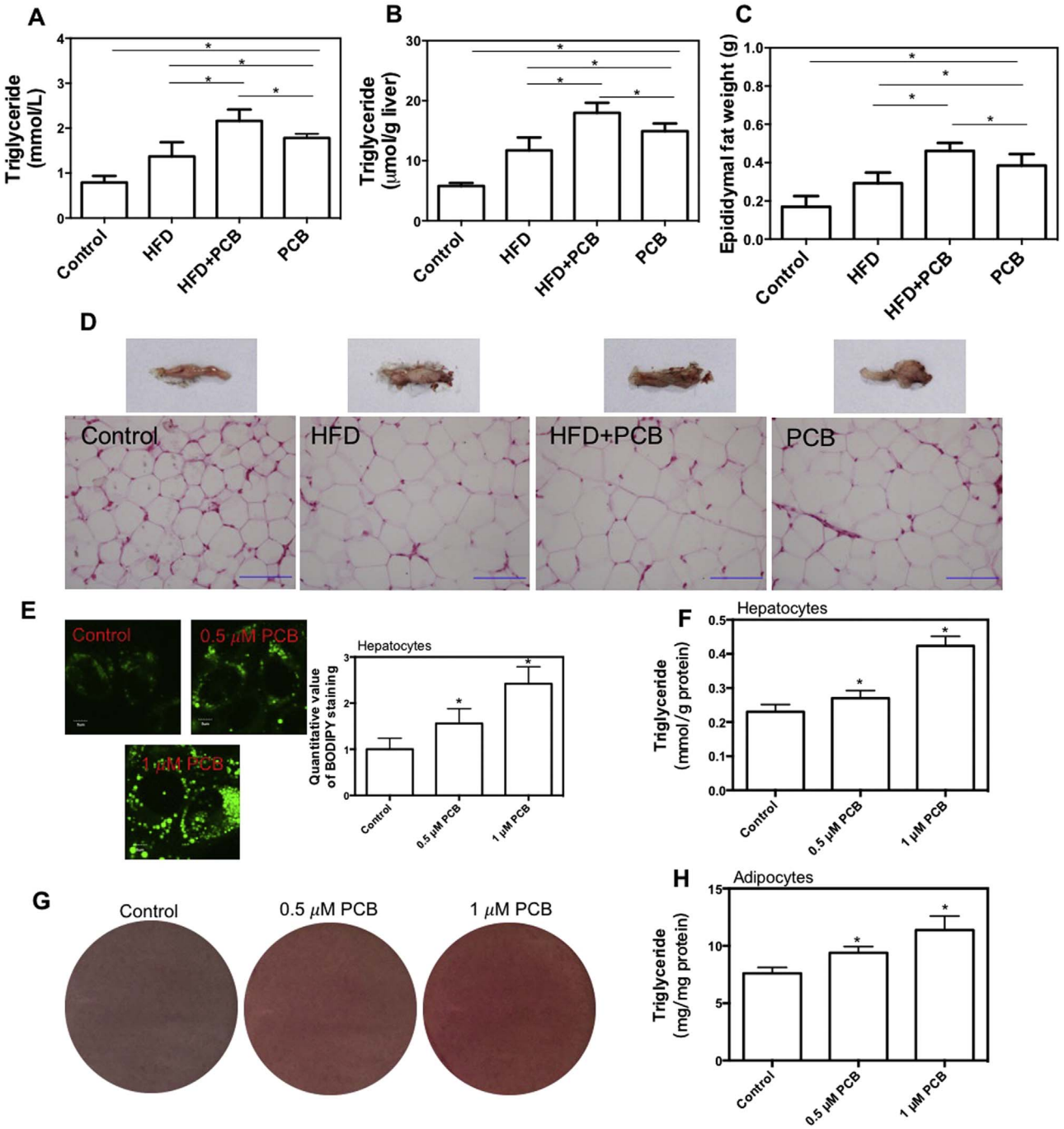

Fig. 2. Effect of PCB-153 on lipid accumulation in vivo and in vitro. Mice were fed high fat diet (HFD) and drank water containing PCB-153. At the end of the experiment, serum (A) and liver (B) triglyceride (TG) content was determined to assess lipid accumulation in circulation and livers. Epididymal fat weight was weighed (C) and HE staining of adipose was conducted (D) to evaluate lipid accumulation in adipose tissue. *$p < 0.05$, significant differences between the two groups. AML-12 hepatocytes were treated by 0.5 and 1 μM PCB-153 for 24 h and cells were stained with BODIPY to observe lipid droplets (E). TG content was also determined in hepatocytes (F). Differentiated 3T3-L1 adipocytes were treated by 0.5 and 1 μM PCB-153 for 24 h and cells were stained with BODIPY to observe lipid droplets (G). TG content was also determined in hepatocytes (H). *$p < 0.05$, significant differences compared with control.

153-resulted reduction of insulin-dependent glucose uptake was markedly inhibited by BMS-345541 and PDTC (Fig. 4A and B, Supplemental Fig. 2A and B), indicating that NF-κB-mediated inflammation was involved in PCB-153-induced insulin resistance.

2.4. PCB-153 resulted in downregulation of HNF1b and oxidative stress

Increased level of ROS is closely related with inflammation and diabetes. Next, we verified whether ROS played a role in PCB-153-induced inflammation and glucose/lipid metabolic disorder. As shown in Fig. 5A and B, PCB-153 resulted in a significant increase in ROS level in both livers and adipose tissues, which was higher than that of HFD group, as reflected by dihydroethidium (DHE) staining. In addition, PCB-153 worsened HFD-resulted increase of ROS level in both livers and adipose tissues (Fig. 5A and B). Moreover, PCB-153 induced a significant increase in ROS level in hepatocytes and adipocytes (Fig. 5C and D). PCB-153 induced the increase of ROS as early as 3 h after the exposure and the ROS level peaked at 24 h after PCB-153 treatment in hepatocytes (Fig. 5E). PCB-153 treatment

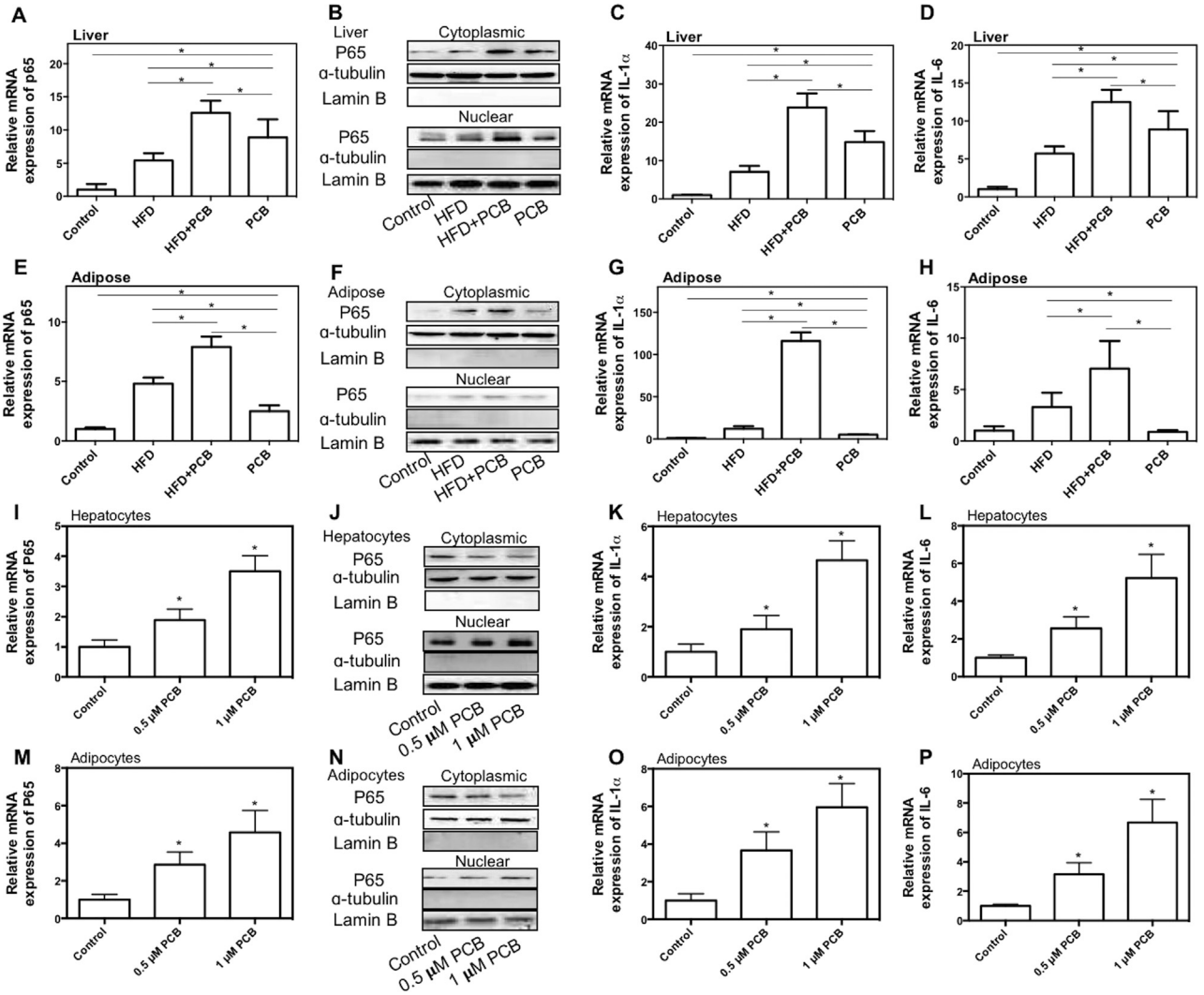

Fig. 3. Effect of PCB-153 on inflammation markers in vivo and in vitro. Mice were fed high fat diet (HFD) and drank water containing PCB-153. At the end of the experiment, mRNA expression of p65 subunit of NF-κB (A and E), nuclear and cytoplasmic protein expression of p65 subunit of NF-κB (B and F), mRNA expression of IL-1α (C and G), and IL-6 (D and H) in livers and adipose tissues were determined. For protein expression, cropped blots were displayed. *$p < 0.05$, significant differences between the two groups. AML-12 hepatocytes were treated by 0.5 and 1 μM PCB-153 for 24 h and mRNA expression of p65 subunit of NF-κB (I), nuclear and cytoplasmic protein expression of p65 subunit of NF-κB (J), mRNA expression of IL-1α (K), and IL-6 (L) were determined. Differentiated 3T3-L1 adipocytes were treated by 0.5 and 1 μM PCB-153 for 24 h and mRNA expression of p65 subunit of NF-κB (M), nuclear protein expression of p65 subunit of NF-κB (N), mRNA expression of IL-1α (O), and IL-6 (P) were determined. For protein expression, cropped blots were displayed. *$p < 0.05$, significant differences compared with control.

decreased glutathione (GSH)/oxidized GSH (GSSG) ratio and increased NADP+/NADPH ratio in hepatocytes (Fig. 5F and G). These results indicated that PCB-153 could induce per se and worsen HFD-resulted oxidative stress.

HNF1b is a member of the hepatocyte nuclear factor family. Glutathione peroxidase (GPx) is an important antioxidant enzyme using GSH as a reductant. In the study, we found that PCB-153 induced a significant decrease of HNF1b and GPx1 mRNA and protein expression in both livers and adipose tissues (Fig. 6A, B, C and D). In addition, PCB-153 worsened HFD-induced decrease of mRNA and protein expression of HNF1b and GPx1 (Fig. 6A, B, C and D). Moreover, PCB-153 resulted in a marked reduction of HNF1b and GPx1 mRNA and protein expression in both AML-12 hepatocytes and 3T3-L1 adipocytes (Fig. 6E, F, G and H). We detected a binding of HNF1b in the promoters of GPx1 under basal condition (Fig. 6I and J). PCB-153 significantly decreased the binding of HNF1b in the promoters of GPx1 (Fig. 6I and J). To evaluate whether HNF1b was involved in PCB-153-induced regulation of redox state, AML-12 cells and 3T3-L1 preadipocytes were transfected with HNF1b plasmids. We showed that upregulation of HNF1b significantly increased GPx1 expression (Fig. 6K, L, M and N). Moreover, overexpression of HNF1b reduced both basal and PCB-153-increased ROS level in hepatocytes and adipocytes (Fig. 6O and P). The treatment of N-acetyl-cysteine (NAC), a potent antioxidant, inhibited PCB-153-induced increase of ROS and decreased basal ROS level (Fig. 6O, P and Q). The results demonstrated that HNF1b functioned as a redox regulator through regulation of GPx1 expression and downregulation of HNF1b/GPx1 played a role in PCB-153-induced increase of ROS.

In the next step, the effect of overexpression of HNF1b and antioxidant treatment on PCB-153-induced glucose/lipid metabolic dysfunction was examined. As shown in Fig. 7A and B, overexpression of HNF1b and NAC treatment significantly inhibited PCB-153-induced increase of p65 expression in hepatocytes and adipocytes. Moreover, overexpression of HNF1b and NAC treatment significantly decreased basal level of TG and PCB-153-induced increase of TG (Fig. 7C and D). Furthermore, overexpression of HNF1b and NAC treatment significantly inhibited PCB-153-resulted decrease of insulin-dependent glucose uptake (Fig. 7E and F). Overexpression of HNF1b increased insulin-dependent glucose uptake under basal condition (Fig. 7E and F). In hepatocytes, overexpression of HNF1b treatment resulted in a

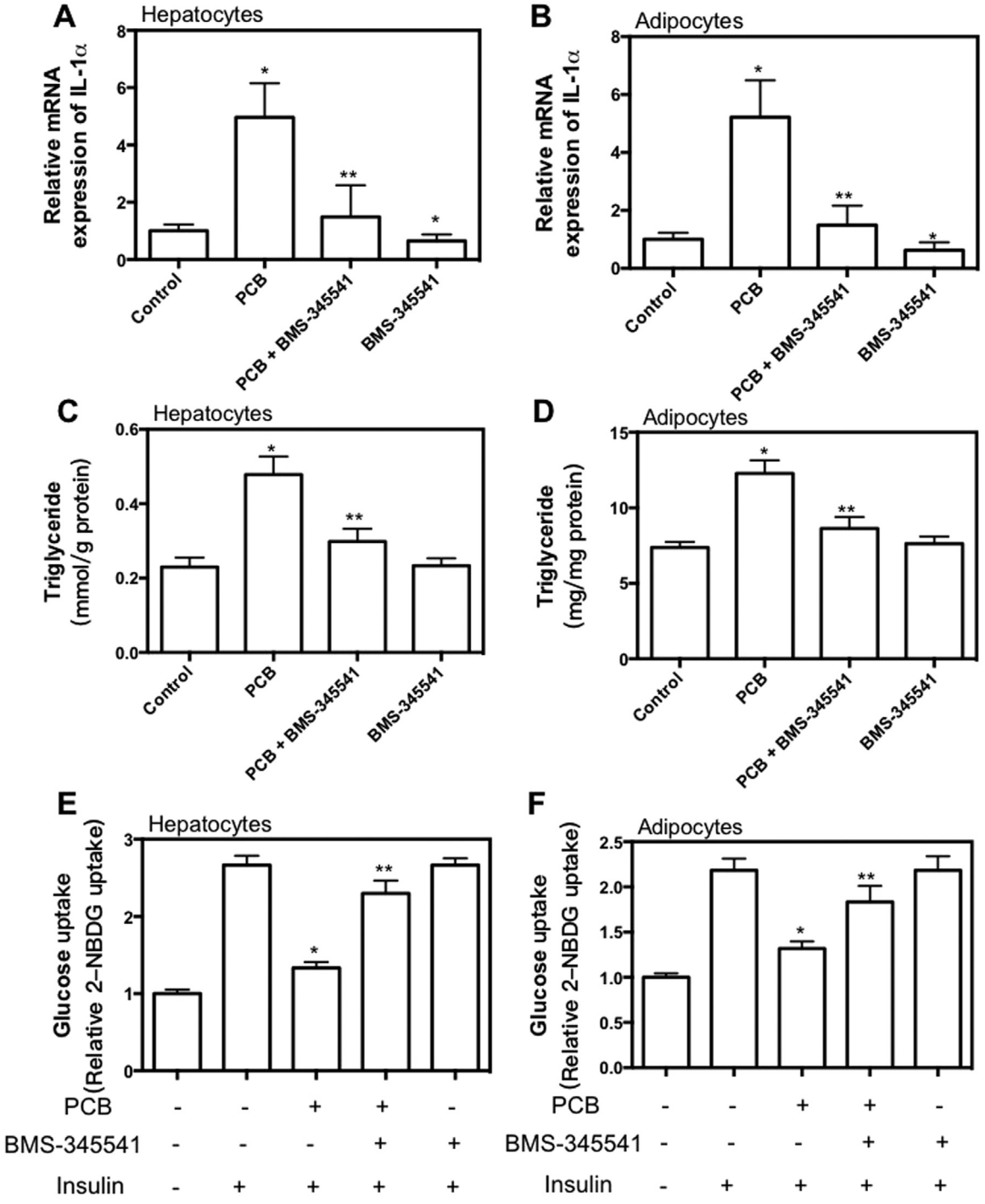

Fig. 4. Role of NF-κB in PCB-153-induced effect on inflammation, lipid accumulation and glucose uptake in hepatocytes and adipocytes. AML-12 hepatocytes and differentiated 3T3-L1 adipocytes were treated by 1 μM PCB-153 for 24 h with or without 10 μM BMS-345541, an inhibitor of NF-κB. mRNA expression of p65 subunit of NF-κB (A and B) were determined using real-time PCR. Results were shown as folds of control. TG content (C and D) and insulin-stimulated glucose uptake (E and F) were determined. *$p < 0.05$, significant differences compared with control. **$p < 0.05$, significant differences compared with PCB.

significant decrease in the expression of sterol regulatory element binding protein (Srebp1), fatty acid synthase (FAS) and acetyl CoA carboxylase (ACC) in the presence or absence of PCB-153 (Fig. 7G, H and I). The results indicated that decrease of HNF1b expression and the increase of ROS was involved in PCB-153-resulted inflammation, lipid accumulation and insulin resistance (Fig. 8).

3. Discussion

Large number of literatures suggest that PCBs are endocrine-disrupting chemicals and PCBs exposure are correlated with obesity, type 2 diabetes and metabolic syndrome [19–23]. However, the mechanism of PCBs-related metabolic disorder is far from completely understood. In the present study, we used PCB-153, an important non-dioxin like PCBs, to study the effect of PCBs on glucose/lipid metabolism. We found that PCB-153 could induce per se and worsen HFD-resulted glucose metabolic dysfunction, as reflected by increase of fasting blood glucose, impairment of glucose and insulin tolerance and decrease of insulin-dependent glucose uptake. Moreover, we found that PCB-153 could induce per se and worsen HFD-resulted increase of TG

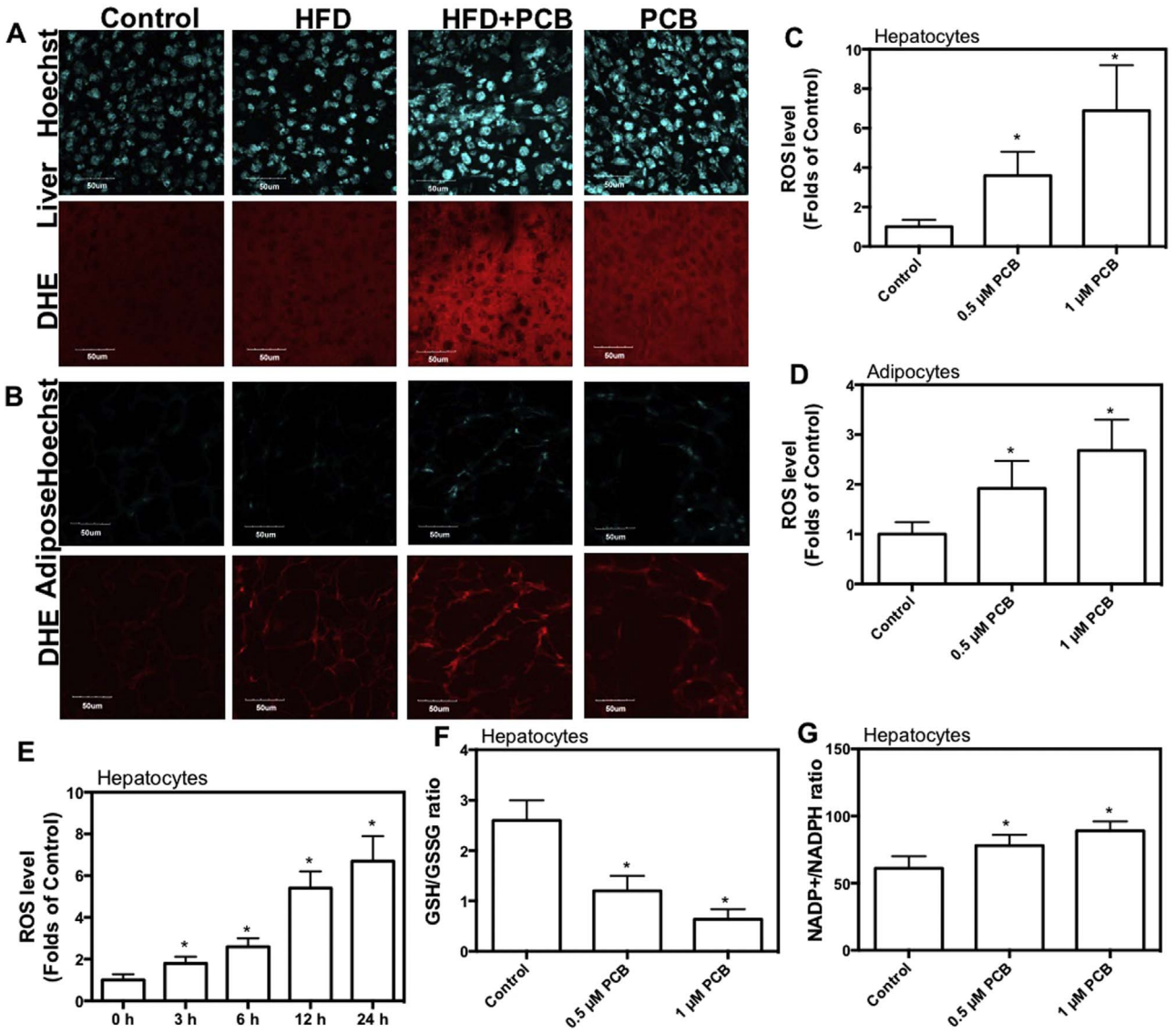

Fig. 5. Effect of PCB-153 on oxidative stress in vivo and in vitro. Mice were fed high fat diet (HFD) and drank water containing PCB-153. At the end of the experiment, frozen sections of livers (A) and adipose tissues (B) were cut and stained with 10 μM dihydroethidium (DHE) to evaluate ROS level. Representative images were captured. AML-12 hepatocytes and differentiated 3T3-L1 adipocytes were treated by 0.5 and 1 μM PCB-153 for 24 h. After that, cells were incubated with 10 μM DHE and analyzed using flow cytometry. ROS level was expressed as folds of control (C and D). 0, 3, 6, 12, and 24 h after the treatment of PCB-153 in hepatocytes, ROS level was determined by DHE staining (E). 24 h after the treatment of PCB-153 in hepatocytes, GSH, GSSG, NADP+ and NADPH content were determined and GSH/GSSG ratio and NADP+/NADPH ratio were shown (F and G). *$p < 0.05$, significant differences compared with control.

in vivo and in vitro, indicating the induction of abnormal lipid metabolism. Previous studies have shown that PCB-153 is a diet-dependent obesogen that worsens nonalcoholic fatty liver disease in mice [18]. The authors found that PCB-153 exacerbated hepatic steatosis, altered adipocytokines and disrupted hepatic lipid metabolism when mice were administered with HFD but not control diet [18]. In contrast, our finding showed that PCB-153 could induce abnormal glucose and lipid metabolism in mice that were administered with normal diet. The discrepancy may be attributed to different exposure routes and doses of PCB-153 intake. Overall, combined with previous literature, our findings suggested that PCB-153 functioned as an endocrine/metabolism-disrupting chemical that induce and exacerbate diet-dependent glucose/lipid metabolic disorder.

To examine the mechanism of PCB-153-induced glucose/lipid metabolic disorder, we investigated the changes of inflammatory regulators in response to PCB-153. PCB-153 has been found to activate NF-κB pathway in macrophages [24]. Liu et al. has shown that PCB-153 induces endothelial cell inflammation through epigenetic regulation of NF-κB subunit p65 [25]. Absence of the NF-κB p50 subunit alters the proliferative and apoptotic changes in mouse liver in the response to PCB-153 [26]. In our study, we found that PCB-153 resulted in diet-dependent or independent p65 NF-κB subunit expression and nuclear translocation, and its downstream targets such as IL-1α and IL-6. NF-κB-mediated inflammation was involved in PCB-153-resulted abnormal glucose/lipid metabolism. In both livers and adipose tissues, the increase of the expression of p65 and IL-1α/6 in response to PCB-153 exposure was higher than that in hepatocytes and adipocytes in vitro. The results indicated that the mechanism of PCB-153-regulated inflammatory response was complicated which could not be reflected in a single cell line. The interaction between tissues or cell types may contribute to PCB-153-resulted inflammation. For example, in tissues, there are plenty of macrophages that may be involved in the inflammation induced by PCB-153.

Oxidative stress has been believed to be associated with inflammation, obesity and type 2 diabetes [27,28]. Previous evidence has shown that PCBs may induce oxidative stress in various cells [29–31].

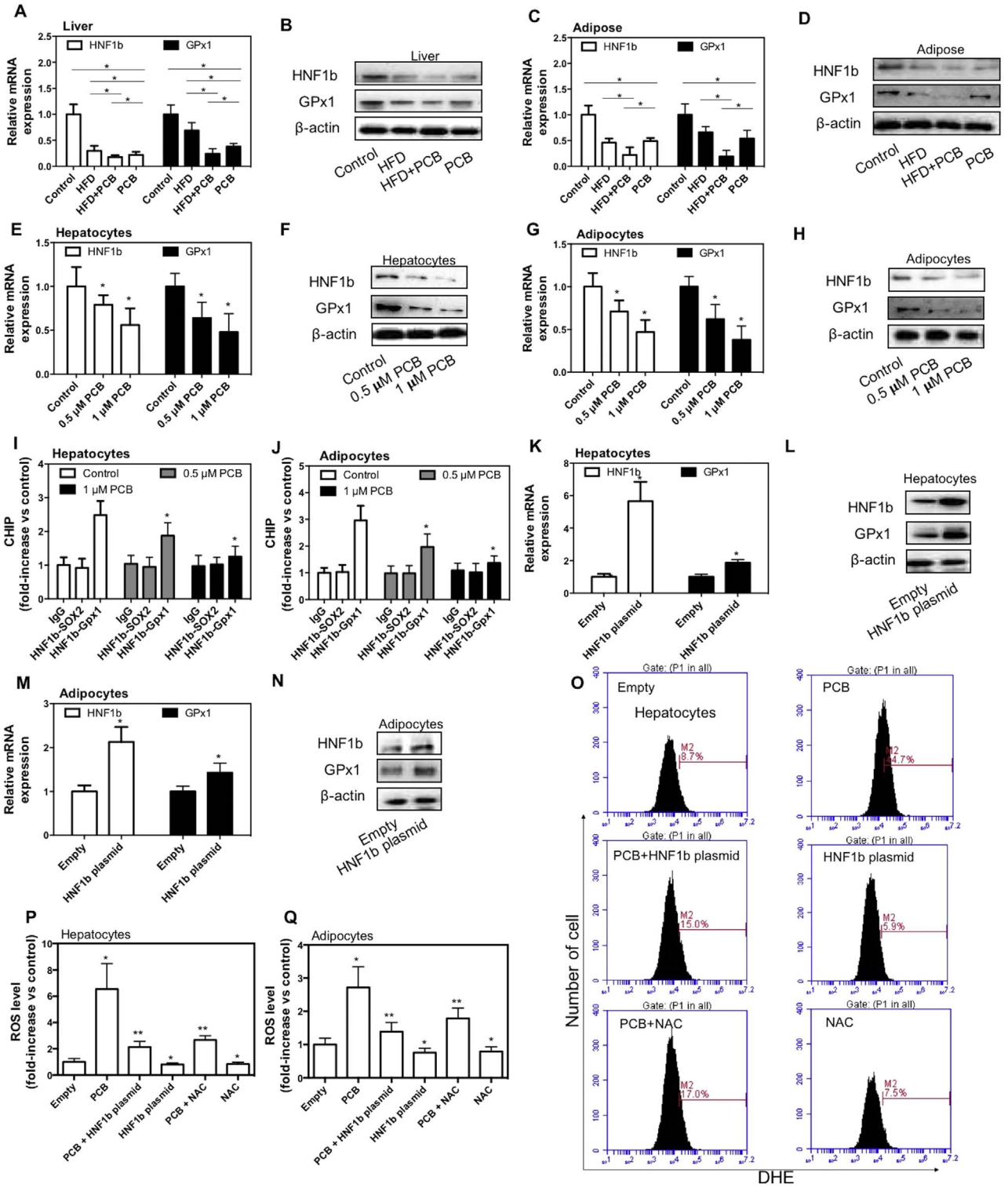

Fig. 6. Effect of PCB-153 on HNF1b and GPx1 expression in vivo and in vitro. Mice were fed high fat diet (HFD) and drank water containing PCB-153. At the end of the experiment, mRNA and protein expression of HNF1b and GPx1 in livers (A and B) and adipose tissues (C and D) were determined. For protein expression, cropped blots were displayed. *$p < 0.05$, significant differences between the two groups. AML-12 hepatocytes and differentiated 3T3-L1 adipocytes were treated by 0.5 and 1 μM PCB-153 for 24 h. After that, mRNA and protein expression of HNF1b and GPx1 in hepatocytes (E and F) and adipocytes (G and H) were determined. HNF1b binding in the promoters of GPx1 in heptatocytes (I) and adipocytes (J) was detected using CHIP assay. For protein expression, cropped blots were displayed. *$p < 0.05$, significant differences compared with control. AML-12 hepatocytes and 3T3-L1 preadipocytes were transfected with HNF1b plasmids. mRNA and protein expression of HNF1b and GPx1 in hepatocytes (K and L) and differentiated adipocytes (M and N) were determined. For protein expression, cropped blots were displayed. *$p < 0.05$, significant differences compared with empty control. Then, hepatocytes and differentiated adipocytes were exposed to 1 μM PCB-153 with or without 500 μM NAC for 24 h. ROS level was determined using DHE staining, analyzed by flow cytometry and expressed as folds of cells transfected with empty plasmids (O, P and Q). *$p < 0.05$, significant differences compared with empty control. **$p < 0.05$, significant differences compared with PCB.

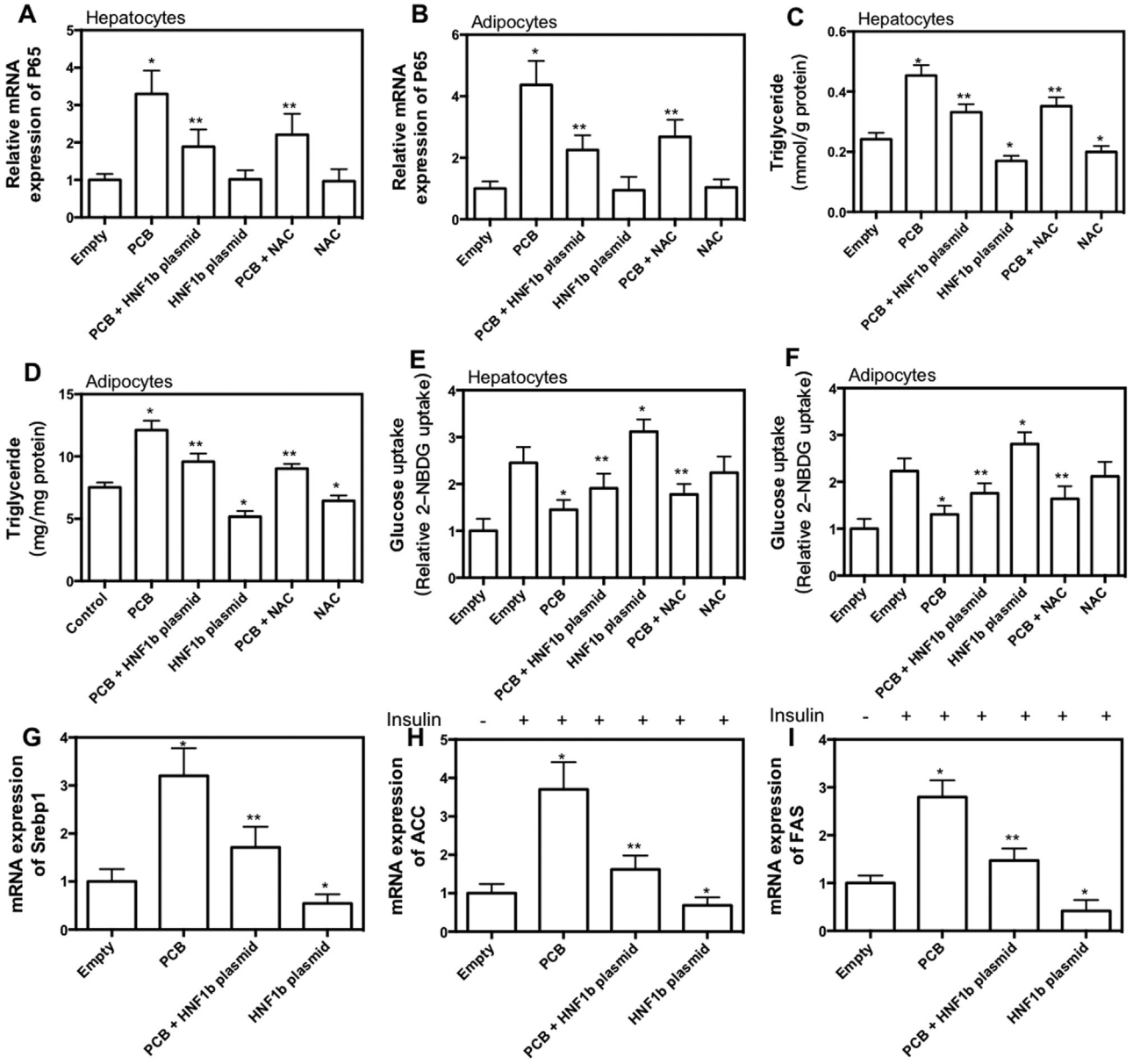

Fig. 7. Role of HNF1b in PCB-153-induced glucose and lipid metabolic disorder. AML-12 hepatocytes and 3T3-L1 preadipocytes were transfected with HNF1b plasmids. Then, hepatocytes and differentiated adipocytes were exposed to 1 μM PCB-153 with or without 500 μM NAC for 24 h. mRNA expression of p65 was determined and shown as folds of control (A and B). TG content (C and D) and insulin-stimulated glucose uptake (E and F) was determined. mRNA expression of Srebp1, ACC and FAS was determined and shown as folds of control (G, H and I). *p < 0.05, significant differences compared with empty control. **p < 0.05, significant differences compared with PCB.

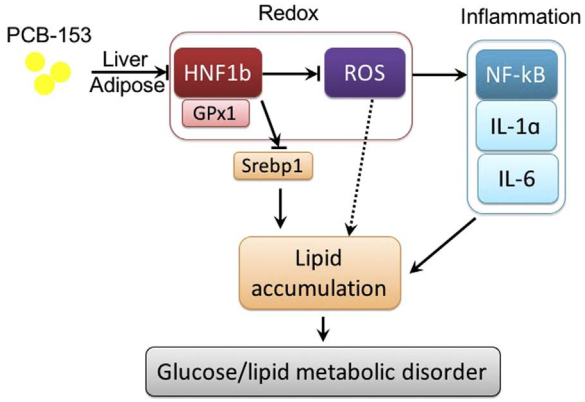

Fig. 8. Schematic figure of the mechanism underlying PCB-153-induced glucose and lipid metabolic disorder.

However, the mechanism of PCBs-exhibited regulation of ROS generation and antioxidant response is unclear. In the current study, we confirmed that PCB-153 could induce and worsen diet-dependent increase of ROS in vivo and in vitro. The intracellular ratio of NADP + to NADPH and GSH to GSSG are believed to be critical regulators of the oxidative stress response [32]. PCB-153 resulted in imbalance of NADP+ to NADPH and GSH to GSSG, indicating that PCB-153 exposure contributed to evident oxidative stress. Antioxidant NAC treatment significantly inhibited PCB-153-induced inflammation, lipid accumulation and insulin resistance, indicating that oxidative stress played an important role in the metabolism-disturbing effect of PCB-153.

Furthermore, we focused on the role of a new redox regulator, HNF1b. HNF1b is a transcription factor that regulates tissue-specific gene expression in the kidney, liver, pancreas, adipose and other tissues [33]. Mutations of the gene encoding HNF1b cause maturity-onset diabetes of the young, type 5 (MODY5) which is characterized by

early-onset diabetes mellitus and congenital malformations of the kidney, pancreas, and genital tract [34–36]. HNF1b and HNF1a have a similar structure with a DNA binding domain consisting of an N-terminal dimerization domain, a Pit-1/Oct-1/Unc-86 (POU) domain and homeodomain that mediate DNA binding, and a C-terminal transcriptional activation domain [37]. HNF1a and HNF1b recognize and bind to the consensus sequence 5′-GTTAATNATTAAC-3′ as homodimers or heterodimers, and activate or repress target gene expression [37]. Our results showed that HNF1b played an antioxidant role through transcriptional regulation of GPx1 and upregulation of HNF1b inhibited PCB-153-induced oxidative stress, inflammation and glucose/lipid metabolic disorder. A previous study has reported that HNF1b promotes glucose uptake and glycolytic activity in ovarian clear cell carcinoma [38]. HNF1b is the target of miR-802 in the development of obesity-associated impairment of glucose metabolism [39]. Quan et al. have reported that HNF1b protects against fatty acid-induced inhibition of Akt signaling, expression of pancreatic duodenal homeobox-1 and glucose transporter 2 and ROS generation in β cells [40]. Our results further confirmed that upregulation of HNF1b could decrease Srebp1, ACC and FAS, key regulators of de novo fatty acid synthesis and extension of fatty acids [41], decrease TG content and increase insulin-dependent glucose uptake in hepatocytes. In combination with previous findings, our results suggest that HNF1b plays a fundamental role in the regulation of redox balance and glucose and lipid metabolism, which is responsive to PCB-153.

Despite of the new findings, our present study has limitations in clarifying the exact relationship between the actual exposure dose of PCB-153 and its biological effects. Because of the high lipophilicity, the water solubility of PCB-153 is only in the range of 0.0012–0.0095 mg/L. Considering this low water solubility, the concentration of PCB-153 in drinking water in our study would not be as high as 4 mg/L. Thus, the mice could not get 1 mg/kg PCB-153 orally each day. It means that the potency of PCB-153 to generate the indicated effects is much higher which is then even more important for risk assessment. However, PCB-153 can partition between water, glass surface and other potential compartments. This may increase the possibility that mice got in contact with non-dissolved PCB-153 orally via care of their body, inhalation, dermal contact and so forth. Moreover, in the cell culture experiments, 0.5–1 μM concentrations are used which are again too high to be solubilized in water. However, the cell culture media could contain ingredients which support the solubility of PCB-153 and its bioavailability for the cells. This may reflect relative higher level of PCB-153 that cells may be exposed to which would not happen in actual environment. All these concerns should be addressed by strictly controlling the exposure route and detection of in vivo PCB-153 concentration in circulation in the further studies.

Overall, we found that PCB-153 downregulated HNF1b and GPx1 expression, increased ROS level, enhanced NF-κB-mediated inflammation, and contributed to abnormal lipid accumulation and glucose metabolism. Further studies are also needed to clarify the mechanism of PCB-153-induced regulation of HNF1b and to explore the pathways responsible for HNF1b-exhibited regulation of redox and glucose/lipid metabolism. In conclusion, our results suggest that downregulation of HNF1b and activation of ROS/NF-κB-mediated inflammation play an important role in PCB-153-induced glucose/lipid metabolic disorder.

4. Materials and methods

IBMX were purchased from Santa Cruz Biotechnology. DHE and BODIPY were purchased from Invitrogen. Insulin, the inhibitor and most of the chemicals and reagents used in this study were procured from Sigma.

4.1. Animal treatment

60 male C57 mice were purchased from the Animal Centre of Fourth Military Medical University. All experiments were performed according to the procedures approved by Fourth Military Medical University Animal Care and Use Committee. The mice were housed under temperature (23 ± 2 °C) and humidity (55 ± 5%) condition with a standard light cycle (12 h light/dark).

Mice were randomly divided into four groups: Control, high fat diet (HFD) group, HFD + PCB-153 group, and PCB-153 group. Mice in Control and PCB-153 groups were fed normal diet. Mice in HFD and HFD + PCB-153 groups were fed diet contain high fat (45 kcal % fat). Mice in HFD + PCB-153 group and PCB-153 groups drank water containing 4 mg/L PCB-153. Each mouse drank approximately 4–5 ml water and the mount of PCB-153 that each mouse took in was about 1 mg/kg/day. The experimental period was 3 months. Fasted and refed blood glucose was measured. At the end, the mice were fasted overnight and anesthetized with sodium pentobarbital, blood samples were collected, epididymal adipose tissues were weighed, frozen sections of liver and adipose tissue were cut, and then liver and adipose tissues were frozen in liquid nitrogen and then stored at −80 °C.

4.2. Intraperitoneal glucose tolerance test and intraperitoneal insulin tolerance test

Intraperitoneal glucose tolerance test (IPGTT) and intraperitoneal insulin tolerance test (IPITT) were conducted to assess the metabolic activity in response to glucose or insulin load. Mice were fasted for 12 h, and basal level of blood glucose was measured using tail blood drops. Then, mice were intraperitoneally injected with D-glucose (Sigma, 1 g/kg), or insulin (Novolin R, 0.75 U/kg body weight). Blood glucose level at 30, 60, and 120 min time points was measured using blood samples dropped from tails.

4.3. Cell culture and treatment

AML-12 cells and 3T3-L1 cells were purchased from the Cell Bank of the Chinese Academy of Medical Sciences (Shanghai, China). AML-12 cells were cultured in DMEM/F-12 medium containing 10% fetal bovine serum (FBS). For the treatment, cells were incubated with 0.5 or 1 μM PCB-153 in serum-free DMEM/F-12 medium. Preadipocyte 3T3-L1 cells were cultured in DMEM containing 10% fetal calf serum (FCS). Adipogenic differentiation of 3T3-L1 cells was induced by MDI cock tail. In brief, 2 days post confluence (Day 0), 3T3-L1 preadipocytes were stimulated with 0.5 mM isobutylmethylxanthine (IBMX), 1 μM dexamethasone, and 167 nM insulin in DMEM containing 10% FBS (DMI differentiation medium) for 2 days (Day 2). Cells were then maintained in a 10% FBS/DMEM medium with 167 nM insulin for another 2 days (D4) and then cultured in 10% FBS/DMEM medium for an additional 4 days (D8), at which time more than 90% of cells became mature adipocytes with lipid-filled droplets. For the treatment, differentiated 3T3-L1 cells were exposed to 0.5 or 1 μM PCB-153 in serum-free DMEM medium. All media contained penicillin (100 U/ml) and streptomycin (100 μg/ml). The cells were maintained at 37 °C in a humidified 5% CO_2 atmosphere.

4.4. Transfection of plasmids

Cells (5×10^5 cells/ml) were plated into 6-well or 96-well plates. The cells were transiently co-transfected with the HNF1b plasmids (GeneChem, Shanghai, China) using Turbofect Transfection Reagents (Thermo Scientific, USA) according to the manufacturer's protocol. Briefly, serum-free DMEM medium containing 4 μg p-HNF1b or empty plasmids was mixed with the Turbofect Transfection Reagents and added to the cells. After 4 h, the cells were incubated with DMEM medium containing 10% FBS. After 48 h, the cells were treated with 1 μM PCB-153 in serum-free DMEM medium for 24 h.

Table 1
Primers used in the study.

Genes	Forward	Reverse
β-actin	5′-AGGCCAACCGTGAAAAGATG-3′	5′-TGGCGTGAGGGAGAGCATAG-3′
p65	5′-ACAGACCCAGGAGTGTTCACAGA-3′	5′-CATGGACACACCCTGGTTCAG-3′
IL-1α	5′-CCCGTGTTGCTGAAGGAG-3′	5′-ACTTTGTTCTTTGGTGGC-3′
Il-6	5′-TTCCAATGCTCTCCTAAC-3′	5′-TGACCACAGTGAGGAATG-3′
HNF1b	5′-CGACGACTATGACACTCC-3′	5′-TGTTGCATGTATCCCTTG-3′
GPx1	5′-GAAGCGTCTGGGACCTCG-3′	5′-CCAGGTCGGACGTACTTG-3′
Srebp1	5′-GCCCACAATGCCATTGAGA-3′	5′-CAGGTCTTTGAGCTCCACAATCT-3′
ACC	5′-CGCTCAGGTCACCAAAAAGAAT-3′	5′-GTCCCGGCCACATAACTGAT-3′
FAS	5′-CCTGGATAGCATTCCGAACCT-3′	5′-AGCACATCTCGAAGGCTACACA-3′

4.5. Lipid accumulation

Triglyceride (TG) content in serum and liver tissues and PCB-153-treated cells were determined using a commercial assay kit (Nanjing Jiancheng Company, China) according to the manufacture's instruction. Epididymal fat mass were captured and HE staining was conducted to observe adipocyte size. AML-12 cells were fixed with 4% paraformaldehyde for 30 min and then stained with 3.5 ng/ml BODIPY (3922) (room temperature, 20 min) to detect lipid droplet. Images were captured using a confocal microscope (Olympus). Differentiated 3T3-L1 cells were fixed with 4% paraformaldehyde for 30 min, rinsed with water, and then stained with Oil Red O solution (6 parts of saturated Oil Red O dye in isopropanol +4 parts of water) for 30 min. Cells were washed by water to remove excessive dye. Lipid accumulation in cells was observed under a light microscope (Olympus).

4.6. Glucose uptake

Glucose uptake was measured by a fluorescent glucose 2-(N-(7-nitrobenz-2-oxa-1,3-diazol-4-yl)amino)-2-deoxyglucose (2-NBDG) method using a glucose uptake assay kit (Cayman Chemical, USA) according the manufacturer's protocols. Cells were treated with PCB-153 in serum-free DMEM medium. Then, the cells were incubated with 2-NBDG in the presence or absence of 100 nM insulin at 37 °C for 30 min. 2-NBDG content was determined using a microplate fluorimeter (Infinite M200; Tecan, Hillsborough, NC).

4.7. ROS level

For the detection of ROS level in tissues, frozen liver and adipose tissues were incubated with 10 μM dihydroethidium (DHE) for 30 min in dark. Images were captured using a laser scanning confocal microscope (Olympus). For the detection of ROS level in cells, cells were suspended in serum-free culture medium and then incubated with 10 μM DHE at 37 °C for 30 min in dark. After washing with PBS, cells were analyzed using flow cytometry (BD, C6, USA).

4.8. NADP+ and NADPH determination

Hepatocytes were lysed in the NADP Extraction Buffer supplied with the Fluoro NADP/NADPH Detection Kit (Cell Technology, USA). Extracts were analyzed to quantitate the NADP+/NADPH ratio according to the manufacturer's instructions.

4.9. GSH and GSSG determination

GSH and GSSG contents were detected using GSH and GSSG Assay Kit (Beyotime Biotechnology, Nantong, China) according to the manufacturer's protocol. The cells were frozen and thawed twice with liquid nitrogen in a water bath at 37 °C and centrifuged at 10000*g* for 10 min at 4 °C. The supernatant was used for GSH and GSSG determination. Absorbance was measured at 450 nm using a microplate reader (Infinite M200; Tecan, Hillsborough, NC).

4.10. Real-time PCR

Total RNA was isolated from tissues and cells using RNA Isolation Assay Kit (TIANGEN, China). 500 ng of RNA was used to reversely transcribed into cDNA using TaKaRa PrimeScript™ RT-PCR Kit (TaKaRa, China). 1 μl cDNA was used to perform Real-time PCR in 20 μl reaction mixtures with SYBR Green PCR kit (Thermo Scientific, IL, USA) sing a CFX96 real-time PCR system (BioRad, USA). The PCR reaction conditions were as follows: initial denaturation at 95 °C for 10 min followed by 30 cycles at 95 °C for 1 min, annealing at 53 °C for 1 min, extension at 72 °C for 1 min, and final extension at 72 °C for 5 min. The relative amount of RNA was quantified using the comparative cycle threshold (C_T) ($2^{-\Delta\Delta}CT$) method. β-actin was used as internal controls. Results were expressed as folds of control. Primers used were shown in Table 1.

4.11. ChIP-PCR assay

After the PCB treatment, HNF1b binding in the promoters of GPx1 was assessed by a ChIP assay using the Chromatin Immunoprecipitation Assay kit (Thermo Scientific, USA) according to the manufacturer's protocols. Subsequent PCR was conducted as detailed above. Primers of SOX2 encoded by gene on chromosome 3 (the same with GPx1) were used as negative control.

4.12. Western blot

Total protein was separated using RIPA lysis buffer (TIANGEN, China). Nuclear and cytoplasmic protein was extracted using a Nuclear Extraction Assay kit (ThermoFisher Scientific, USA). Protein concentration was determined using BCA method (Thermo Scientific, IL, USA). Equal volumes of protein extraction and loading buffer were mixed and separated using SDS-PAGE on 10% polyacrylamide gels. Separated samples were transferred onto nitrocellulose (NC) membranes. After blocking in 8% fat-free milk for 1 h at room temperature, membranes were incubated with primary antibodies at 4 °C overnight. After washing for four times, the membranes were incubated in the appropriate HRP-conjugated secondary antibody at 37 °C for 30 min. Protein bands were detected using chemiluminescent reagents according to the manufacturer's protocol and observed using an image analyzer Quantity One System (Bio-Rad). The protein quantifications were adjusted for the corresponding β-actin level.

5. Statistical analysis

Results were expressed as the means ± SEM and analyzed by one-way analysis of variance (ANOVA) followed by the Newmane Keuls multiple-comparison post hoc test using Graph-Pad Prism software. Data were considered statistically significant for $p < 0.05$.

Conflict of interest statement

The authors declare that there are no conflicts of interest.

Author contribution

H.W. conducted the experiments, analyzed the data and wrote the paper; W.Y. conducted the experiments, analyzed the data and wrote the paper; X.W. designed and conducted the experiments, analyzed the data and wrote the paper; C.H. designed the experiments and wrote the paper; F.M. conducted the experiments and analyzed the data; rote the paper; J.M. conducted the experiments and analyzed the data; J.P. conducted the experiments and analyzed the data; J.L. conducted the experiments and analyzed the data; N.L. conducted the experiments and analyzed the data; X.Z. conducted the experiments and analyzed the data.

Acknowledgments

This work was supported by National Natural Science Foundation of China (No. 31400724 and No. 21677176).

Appendix A. Supporting information

Supporting information associated with this article can be found in the online version at doi:10.1016/j.redox.2017.02.026.

References

[1] S. Wild, G. Roglic, A. Green, R. Sicree, H. King, Global prevalence of diabetes: estimates for the year 2000 and projections for 2030, Diabetes Care 27 (2004) 1047–1053.
[2] G. Roglic, et al., The burden of mortality attributable to diabetes: realistic estimates for the year 2000, Diabetes Care 28 (2005) 2130–2135.
[3] C.E. Eades, E.F. France, J.M. Evans, Prevalence of impaired glucose regulation in Europe: a meta-analysis, Eur. J. Public Health 26 (2016) 699–706. http://dx.doi.org/10.1093/eurpub/ckw085.
[4] C. Liu, et al., Associations between long-term exposure to ambient particulate air pollution and type 2 diabetes prevalence, blood glucose and glycosylated hemoglobin levels in China, Environ. Int. 92–93 (2016) 416–421. http://dx.doi.org/10.1016/j.envint.2016.03.028.
[5] S. Xiao, et al., Air pollution and blood lipid markers levels: estimating short and long-term effects on elderly hypertension inpatients complicated with or without type 2 diabetes, Environ. Pollut. (Barking, Essex: 1987) 215 (2016) 135–140. http://dx.doi.org/10.1016/j.envpol.2016.05.007.
[6] D.H. Lee, et al., Associations of persistent organic pollutants with abdominal obesity in the elderly: the Prospective Investigation of the Vasculature in Uppsala Seniors (PIVUS) study, Environ. Int. 40 (2012) 170–178. http://dx.doi.org/10.1016/j.envint.2011.07.010.
[7] H.W. Vallack, et al., Controlling persistent organic pollutants-what next?, Environ. Toxicol. Pharmacol. 6 (1998) 143–175.
[8] D.H. Lee, et al., Low dose of some persistent organic pollutants predicts type 2 diabetes: a nested case-control study, Environ. Health Perspect. 118 (2010) 1235–1242. http://dx.doi.org/10.1289/ehp.0901480.
[9] A. Debost-Legrand, et al., Prenatal exposure to persistent organic pollutants and organophosphate pesticides, and markers of glucose metabolism at birth, Environ. Res. 146 (2016) 207–217. http://dx.doi.org/10.1016/j.envres.2016.01.005.
[10] S. Mostafalou, Persistent organic pollutants and concern over the link with insulin resistance related metabolic diseases, Rev. Environ. Contam. Toxicol. 238 (2016) 69–89. http://dx.doi.org/10.1007/398_2015_5001.
[11] D.H. Lee, Persistent organic pollutants and obesity-related metabolic dysfunction: focusing on type 2 diabetes, Epidemiol. Health 34 (2012) e2012002. http://dx.doi.org/10.4178/epih/e2012002.
[12] D.H. Lee, et al., Polychlorinated biphenyls and organochlorine pesticides in plasma predict development of type 2 diabetes in the elderly: the prospective investigation of the vasculature in Uppsala Seniors (PIVUS) study, Diabetes care 34 (2011) 1778–1784. http://dx.doi.org/10.2337/dc10-2116.
[13] J.P. Arrebola, et al., Historical exposure to persistent organic pollutants and risk of incident hypertension, Environ. Res. 138 (2015) 217–223. http://dx.doi.org/10.1016/j.envres.2015.02.018.
[14] P. Langer, et al., Obesogenic and diabetogenic impact of high organochlorine levels (HCB, p,p′-DDE, PCBs) on inhabitants in the highly polluted Eastern Slovakia, Endocr. Regul. 48 (2014) 17–24.
[15] S.L. Gray, A.C. Shaw, A.X. Gagne, H.M. Chan, Chronic exposure to PCBs (Aroclor 1254) exacerbates obesity-induced insulin resistance and hyperinsulinemia in mice, J. Toxicol. Environ. Health Part A 76 (2013) 701–715. http://dx.doi.org/10.1080/15287394.2013.796503.
[16] V. Arsenescu, R.I. Arsenescu, V. King, H. Swanson, L.A. Cassis, Polychlorinated biphenyl-77 induces adipocyte differentiation and proinflammatory adipokines and promotes obesity and atherosclerosis, Environ. Health Perspect. 116 (2008) 761–768. http://dx.doi.org/10.1289/ehp.10554.
[17] A.E. Silverstone, et al., Polychlorinated biphenyl (PCB) exposure and diabetes: results from the Anniston Community Health Survey, Environ. Health Perspect. 120 (2012) 727–732. http://dx.doi.org/10.1289/ehp.1104247.
[18] B. Wahlang, et al., Polychlorinated biphenyl 153 is a diet-dependent obesogen that worsens nonalcoholic fatty liver disease in male C57BL6/J mice, J. Nutr. Biochem. 24 (2013) 1587–1595. http://dx.doi.org/10.1016/j.jnutbio.2013.01.009.
[19] G. Zong, P. Grandjean, X. Wang, Q. Sun, Lactation history, serum concentrations of persistent organic pollutants, and maternal risk of diabetes, Environ. Res. 150 (2016) 282–288. http://dx.doi.org/10.1016/j.envres.2016.06.023.
[20] Y. Song, et al., Endocrine-disrupting chemicals, risk of type 2 diabetes, and diabetes-related metabolic traits: a systematic review and meta-analysis, J. Diabetes 8 (2016) 516–532. http://dx.doi.org/10.1111/1753-0407.12325.
[21] N. Chevalier, P. Fenichel, Endocrine disruptors: a missing link in the pandemy of type 2 diabetes and obesity?, Presse Med. (Paris, France: 1983) 45 (2016) 88–97. http://dx.doi.org/10.1016/j.lpm.2015.08.008.
[22] M. Pavuk, et al., Predictors of serum polychlorinated biphenyl concentrations in Anniston residents, Sci. Total Environ. 496 (2014) 624–634. http://dx.doi.org/10.1016/j.scitotenv.2014.06.113.
[23] T.K. Jensen, et al., Polychlorinated biphenyl exposure and glucose metabolism in 9-year-old Danish children, J. Clin. Endocrinol. Metab. 99 (2014) E2643–E2651. http://dx.doi.org/10.1210/jc.2014-1683.
[24] A. Santoro, et al., Polychlorinated biphenyls (PCB 101, 153, and 180) impair murine macrophage responsiveness to lipopolysaccharide: involvement of NF-kappaB pathway, Toxicol. Sci.: Off. J. Soc. Toxicol. 147 (2015) 255–269. http://dx.doi.org/10.1093/toxsci/kfv127.
[25] D. Liu, J.T. Perkins, M.C. Petriello, B. Hennig, Exposure to coplanar PCBs induces endothelial cell inflammation through epigenetic regulation of NF-kappaB subunit p65, Toxicol. Appl. Pharmacol. 289 (2015) 457–465. http://dx.doi.org/10.1016/j.taap.2015.10.015.
[26] Z. Lu, E.Y. Lee, L.W. Robertson, H.P. Glauert, B.T. Spear, Effect of 2,2′,4,4′,5,5′-hexachlorobiphenyl (PCB-153) on hepatocyte proliferation and apoptosis in mice deficient in the p50 subunit of the transcription factor NF-kappaB, Toxicol. Sci.: Off. J. Soc. Toxicol. 81 (2004) 35–42. http://dx.doi.org/10.1093/toxsci/kfh193.
[27] X. Wang, C. Hai, redox modulation of adipocyte differentiation: hypothesis of "Redox Chain" and novel insights into intervention of adipogenesis and obesity, Free Radic. Biol. Med. 89 (2015) 99–125. http://dx.doi.org/10.1016/j.freeradbiomed.2015.07.012.
[28] X. Wang, C.X. Hai, ROS acts as a double-edged sword in the pathogenesis of type 2 diabetes mellitus: is Nrf2 a potential target for the treatment?, Mini Rev. Med. Chem. 11 (2011) 1082–1092.
[29] F. Wu, Y. Zheng, J. Gao, S. Chen, Z. Wang, Induction of oxidative stress and the transcription of genes related to apoptosis in rare minnow (Gobiocypris rarus) larvae with Aroclor 1254 exposure, Ecotoxicol. Environ. Saf. 110 (2014) 254–260. http://dx.doi.org/10.1016/j.ecoenv.2014.09.012.
[30] B.J. Newsome, et al., Green tea diet decreases PCB 126-induced oxidative stress in mice by up-regulating antioxidant enzymes, J. Nutr. Biochem. 25 (2014) 126–135. http://dx.doi.org/10.1016/j.jnutbio.2013.10.003.
[31] S.H. Park, J.H. Jang, C.Y. Chen, H.K. Na, Y.J. Surh, A formulated red ginseng extract rescues PC12 cells from PCB-induced oxidative cell death through Nrf2-mediated upregulation of heme oxygenase-1 and glutamate cysteine ligase, Toxicology 278 (2010) 131–139. http://dx.doi.org/10.1016/j.tox.2010.04.003.
[32] W. Ying, NAD+/NADH and NADP+/NADPH in cellular functions and cell death: regulation and biological consequences, Antioxid. Redox Signal. 10 (2008) 179–206. http://dx.doi.org/10.1089/ars.2007.1672.
[33] E.L. Edghill, C. Bingham, S. Ellard, A.T. Hattersley, Mutations in hepatocyte nuclear factor-1beta and their related phenotypes, J. Med. Genet. 43 (2006) 84–90. http://dx.doi.org/10.1136/jmg.2005.032854.
[34] T.H. Lindner, et al., A novel syndrome of diabetes mellitus, renal dysfunction and genital malformation associated with a partial deletion of the pseudo-POU domain of hepatocyte nuclear factor-1beta, Hum. Mol. Genet. 8 (1999) 2001–2008.
[35] C. Bellanne-Chantelot, et al., Clinical spectrum associated with hepatocyte nuclear factor-1beta mutations, Ann. Intern. Med. 140 (2004) 510–517.
[36] F. Beards, et al., Mutations in hepatocyte nuclear factor 1beta are not a common cause of maturity-onset diabetes of the young in the U.K, Diabetes 47 (1998) 1152–1154.
[37] P. Igarashi, X. Shao, B.T. McNally, T. Hiesberger, Roles of HNF-1beta in kidney development and congenital cystic diseases, Kidney Int. 68 (2005) 1944–1947. http://dx.doi.org/10.1111/j.1523-1755.2005.00625.x.
[38] T. Okamoto, et al., Hepatocyte nuclear factor-1beta (HNF-1beta) promotes glucose uptake and glycolytic activity in ovarian clear cell carcinoma, Mol. Carcinog. 54 (2015) 35–49. http://dx.doi.org/10.1002/mc.22072.
[39] J.W. Kornfeld, et al., Obesity-induced overexpression of miR-802 impairs glucose metabolism through silencing of Hnf1b, Nature 494 (2013) 111–115. http://dx.doi.org/10.1038/nature11793.
[40] X. Quan, L. Zhang, Y. Li, C. Liang, TCF2 attenuates FFA-induced damage in islet beta-cells by regulating production of insulin and ROS, Int. J. Mol. Sci. 15 (2014) 13317–13332. http://dx.doi.org/10.3390/ijms150813317.
[41] T. Ishikawa, K. Hwang, D. Lazzarino, P.L. Morris, Sertoli cell expression of steroidogenic acute regulatory protein-related lipid transfer 1 and 5 domain-containing proteins and sterol regulatory element binding protein-1 are interleukin-1beta regulated by activation of c-Jun N-terminal kinase and cyclooxygenase-2 and cytokine induction, Endocrinology 146 (2005) 5100–5111. http://dx.doi.org/10.1210/en.2005-0567.